Effects of Time Delays on Systems Subject to Manual Control

Ronald A. Hess*
NASA Ames Research Center, Moffett Field, California

The results of an experimental study to determine the effects of time delays in manual control systems are presented. A simple, fixed base laboratory simulation facility is used to determine pilot dynamics and tracking performance in a series of single-axis compensatory tracking tasks. In the tasks, three time delay values and three controlled-element dynamics are utilized. The delays were chosen to encompass values encountered in experimental and operational aircraft. The controlled-element dynamics replicate those found in many previous manual control studies, that is, the classical displacement, rate, and acceleration control systems. The experimental effort is complemented with an analytical pilot modeling study in which the parameters of a structural model of the human pilot are adjusted to provide excellent matches to the experimentally determined pilot dynamics (transfer functions). Both the experimental and analytical work indicate that time delays cause significant changes in pilot equalization requirements. In particular, lead generation over and above that required to provide K/s-like pilot-vehicle characteristics near the crossover frequency is indicated with the larger time delays studied. The implications of this lead generation in certain closed-loop command following tasks are discussed with particular emphasis on the development of pilot-induced oscillations.

Introduction

IT is generally recognized that the existence of time delays in manual control systems can lead to degraded performance and even closed-loop instability. This problem is particularly evident in modern flight control systems where time delays are almost unavoidable, due to digital control law implementation[1] and the existence of phase lags associated with higher-order control system dynamics.[2] Recent experimental[1,3,4] and analytical[5] work has documented the contribution of time delays to deficiencies in aircraft handling qualities such as pilot-induced oscillations (PIO). However, to the author's knowledge, no systematic experimental study has been undertaken to determine the effects of time delays on human operator (pilot) dynamics. This paper represents the results of such a study to document the effects of time delays on human-operator controlled-element (pilot-vehicle) transfer functions, relative remnant values, and performance scores with a variety of controlled-element dynamics and time-delay values. In addition to the experimental effort just discussed, analytical pilot modeling results are discussed which utilize a structural model of the human pilot.[6]

Approach

Experimental

Figure 1 shows a block diagram of the tracking task and a sketch of the display format utilized in the experimental/analytical study to be described. As Fig. 1a indicates, the task was signal axis and compensatory in nature and involved nulling the system error by the operator. This error was displayed on a CRT screen as shown in Fig. 1b. A small, spring-restrained, finger-manipulator served as the control stick. The display format, input singal, and controlled-element dynamics were generated on a microprocessor-based laboratory facility. The input for the 100 s tracking runs was a random appearing sum of 13 sinusoids approximating a rectangular spectrum with a 2.0 rad/s cutoff frequency. Details are given in Table 1. The 2.0 rad/s frequency is representative of input cutoff frequencies used in other modeling efforts, e.g., Ref. 7. The task was fixed base in nature. Table 2 lists the controlled-element dynamics and time-delay values used in the experiment. The controlled-element dynamics replicated those found in previous manual control theory and pilot-modeling studies; e.g., Refs. 7 and 8. The range of time delays encompasses values encountered in both experimental[1] and operational[2,9] aircraft. For convenience the time-delay values were chosen as integer multiples (0,4,7) of the 0.0476 s sampling interval of the microprocessor. Since the controlled-element dynamics were implemented digitally, additional delay was encountered. In the case of the K dynamics, the delay was an entire sampling interval; for the K/s and K/s^2 dynamics, it was one-half of the sampling interval.

These different delay values can be explained by considering the difference equations which describe the simulated dynamics. For $Y_c = K$, the appropriate difference equation is

$$m(nT+T) = K\delta(nT) \tag{1}$$

where δ represents the subject's control output, and T is the sampling interval. For $Y_c = K/s$,

$$m(nT+T) = m(nT) + TK\delta(nT) \tag{2}$$

Finally, for $Y_c = K/s^2$, with $x_1 = m$, and $x_2 = \dot{m}$,

$$x_1(nT+T) = x_1(nT) + Tx_2(nT) + (T^2/2)K\delta(nT)$$

$$x_2(nT+T) = x_2(nT) + TK\delta(nT) \tag{3}$$

Now it can be shown[10] that the implementation of Eq. (1) will yield a delay of an entire sampling interval, while that of Eqs. (2) and (3) will yield a delay closely approximating one-half a sampling interval. The controlled-element dynamics/time-delay combinations were presented to each of the four test subjects participating in the experiment in the order shown in Table 2. This ordering, while not random, was chosen to minimize the effects of transfer of training.

The actual experimental procedure was quite simple. Beginning with the first dynamics/delay combination, the

Presented as Paper 83-1523 at the AIAA Guidance and Control Conference, San Diego, Calif., Aug. 9-11, 1982; received Aug. 9, 1982; revision received July 27, 1983. This paper is declared a work of the U.S. Government and therefore is in the public domain.

*Aircraft Guidance and Navigation Branch; presently Associate Professor, Department of Mechanical Engineering, University of California, Davis, Calif. Member AIAA.

Table 1 Sum of sinusoids command input

$$c(t) = \sum_{i=1}^{13} A_i \sin(\omega_i t + \phi_i)$$

i	A_i/A_1	ω_i, rad/s	No. of cycles in 100-s run	ϕ_i
1	1.0	0.18850	3	$\pi/6.5$
2	1.0	0.31416	5	$2\phi_1$
3	1.0	0.50265	8	$3\times\phi_1$
4	1.0	0.87965	14	$4\times\phi_1$
5	1.0	1.44513	23	$5\times\phi_1$
6	1.0	2.13628	34	$6\times\phi_1$
7	0.1	3.07876	49	$7\times\phi_1$
8	0.1	4.20973	67	$8\times\phi_1$
9	0.1	5.78053	92	$9\times\phi_1$
10	0.1	8.23097	131	$10\times\phi_1$
11	0.1	11.24690	179	$11\times\phi_1$
12	0.1	15.77079	251	$12\times\phi_1$
13	0.1	23.93894	381	$13\times\phi_1$

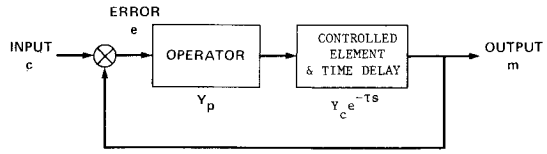

Fig. 1a Diagram of single-axis compensatory tracking task.

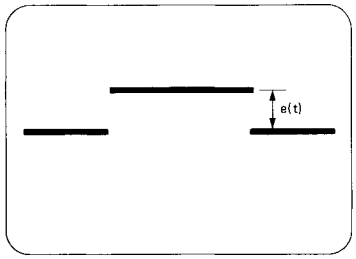

Fig. 1b Display used in tracking task of Fig. 1a.

first subject completed tracking runs until root mean square (rms) error scores reached asymptotic values indicating that the subject was trained sufficiently. Then four data runs were completed in which the following measurements were taken: 1) rms error scores, 2) operator-controlled element transfer functions; i.e., $Y_p Y_c(s)$ in Fig. 1a, and 3) relative remnant values. Relative remnant is a measure of operator linearity and time stationarity and is defined here as the ratio of the power in the error signal at the input frequencies to the total power in the error signal. Thus, the closer the relative remnant value is to unity, the more linear and time invariant are the operator's dynamics.

For inputs consisting of the sum of sinusoids, the magnitude and phase of $Y_p Y_c$ at each of the input frequencies ω_i can be obtained as:

$$|Y_p Y_c(j\omega_i)| = \frac{|M(j\omega_i)|}{|E(j\omega_i)|}$$

$$\angle Y_p Y_c(j\omega_i) = \angle M(j\omega_i) - \angle E(j\omega_i)$$

where $M(j\omega_i)$ and $E(j\omega_i)$ are the periodic Fourier coefficients for the signals $m(t)$ and $e(t)$. Likewise, the relative remnant ρ^2 can be expressed as

$$\rho^2 = \sum_{i=1}^{13} |E(j\omega_i)|^2 \Big/ (1/100) \int_0^{100} e^2(t)\,dt$$

Table 2 Controlled elements and time-delay values

	Controlled elements		
	K	K/s	K/s^2
Time delays, s	0.0476 (4)[a]	0.0238 (7)	0.0238 (3)
	0.238 (8)	0.214 (2)	0.214 (6)
	0.381 (1)	0.357 (5)	–[b]

[a] Number in parentheses represents the order of presentation to operators.
[b] Control was not possible with large delay for K/s^2 dynamics.

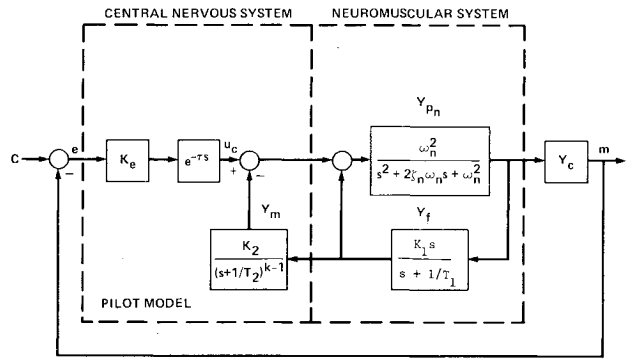

Fig. 2 The structural model of the human pilot.

The frequency domain identification process is unaffected by the presence of time delays in the plant. Indeed, it has long been used to identify similar delays in the pilot himself.[8]

After the four data runs, the first subject moved on to tracking the second dynamics/delay combination, etc., until all the combinations were completed. The process was repeated for each of the subjects. In all, 128 data runs were completed.

Analytical

Figure 2 shows what the author calls a structural model of the human pilot.[6] The model, discussed in detail in Ref. 6, is capable of matching human pilot transfer functions for a wide variety of controlled-element dynamics, including those used in this study. The model has been divided into "central nervous system" and "neuromuscular system" components, a division intended to emphasize the nature of the signal-processing activity involved. System error $e(t)$ is presented to the pilot via a visual display. A constant gain K_e multiplies the signal $e(t)$. A central time delay of τ_0 s is included to account for the effects of latencies in the visual process sensing $e(t)$, motor nerve conduction times, etc. This delay is not to be confused with those which may occur in the controlled element, however. The signal $u_c(t)$ provides a command to a closed-loop system, which consists of a model of the open-loop neuromuscular dynamics of the arm/hand Y_{pn}, and elements Y_f and Y_m which emulate, at least approximately, the combined effects of the muscle spindles and the dynamics associated with higher-level signal processing. Note that all of the pilot's equalization capabilities (generation of lead, lag, etc.) in the model of Fig. 2 occur through the action of the two loop closures around the open-loop neuromuscular system. As pointed out in Ref. 6, this equalization is created by an "internal model" of the controlled-element dynamics valid in the frequency region of open-loop crossover, and explicitly contained in the product $Y_f Y_m$. Nominally, the internal model is parameterized simply by the integer k, which represents the order of the controlled-element dynamics in the region of crossover. For example, for values of $1/T_1$ and $1/T_2$ significantly less than the crossover frequency ω_c (which they will be for the cases here), the product of $Y_f Y_m$ can, in

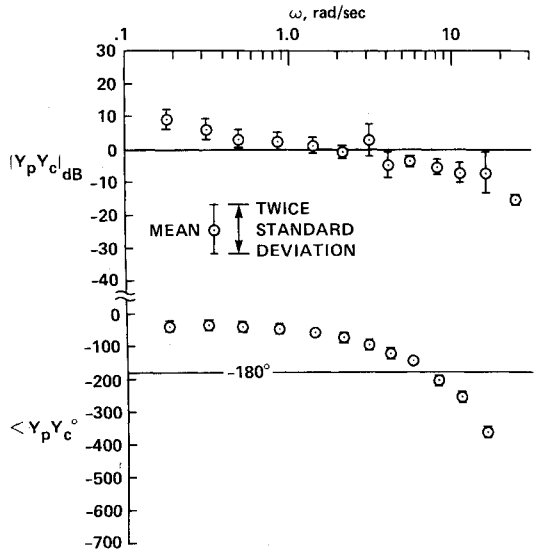

Fig. 3 Human-operator controlled-element transfer function for a single subject. Average of four runs. $Y_c = K$, delay = 0.0474 s.

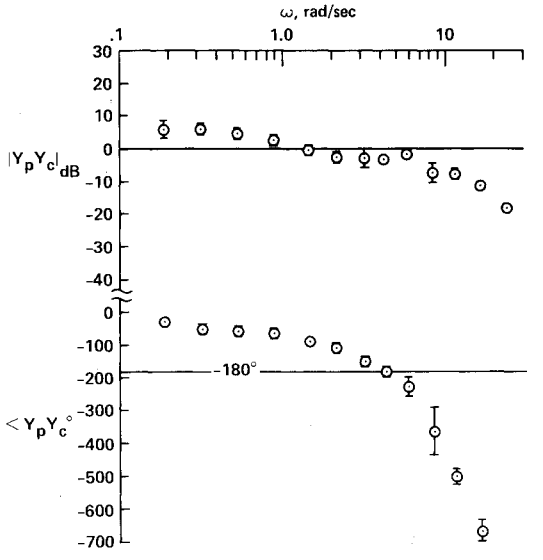

Fig. 4 Human-operator controlled-element transfer function for a single subject. Average of four runs. $Y_c = K$, delay = 0.0381 s.

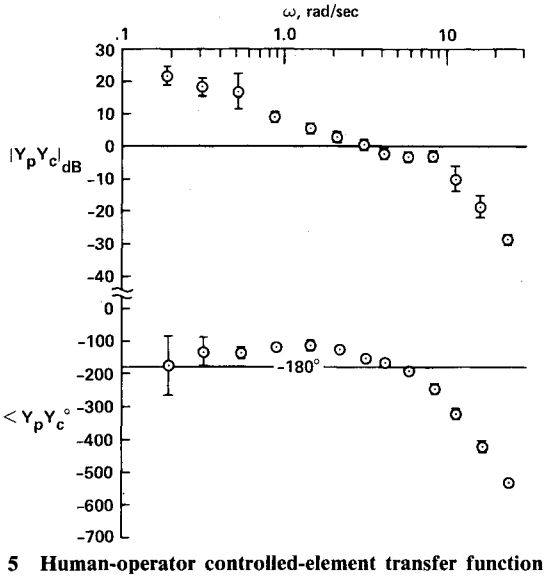

Fig. 5 Human-operator controlled-element transfer function for a single subject. Average of four runs. $Y_c = K/s$, delay = 0.0238 s.

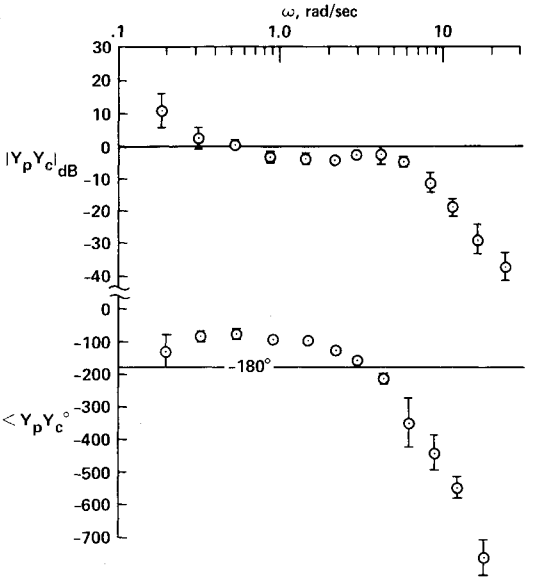

Fig. 6 Human-operator controlled-element transfer function for a single subject. Average of four runs. $Y_c = K/s$, delay = 0.357 s.

the region of crossover, be approximated by

$$Y_f Y_m = \frac{K_1 K_2}{s^{k-1}}$$

Thus, the signal processing implied by $Y_f Y_m$ takes the form of differentiating ($k=0$), multiplication by a constant ($k=1$), and integration ($k=2$), depending upon the order of the controlled-element dynamics in the regions of crossover.

The model has been used to provide a rationale for certain nonlinear pilot control behavior, such as stick pulsing,[11] has served as a framework for studying aspects of motor skill development,[12] and has provided insight into the contribution of manipulator characteristics to pilot-vehicle performance.[13] In this study, the model parameters were adjusted so that the transfer function of the model/controlled-element combination provided a satisfactory match to the experimental transfer functions just discussed for each controlled-element/delay combination.

The structural model of the pilot was chosen in lieu of other mathematical representations, such as the optimal control model,[7] since the former allows a more direct interpretation of pilot equalization activity (e.g., lead generation). This will be an important consideration, as will be seen shortly.

Results

Figures 3-8 exemplify the experimental results for one subject and are representative of the data for the remaining three. These figures show the transfer functions for the combination human operator and controlled element (pilot-vehicle) for each of the controlled elements and the extreme time-delay values. Figure 9 shows the average rms performance and relative remnant scores in addition to the average pilot-vehicle crossover frequencies [frequency at which $Y_p Y_c(j\omega_i) = 1.0$]. Finally, Figs. 10 and 11 show the pilot-vehicle transfer functions obtained from the structural model of Fig. 2, where the model parameters were adjusted in ad hoc fashion to match the data of Figs. 5 and 6.

The most dramatic effect of the time delays is seen in the pilot-vehicle transfer functions. The rms error scores increase with time delay but the increase is quite modest when compared with the magnitude of the delay increment. In addition,

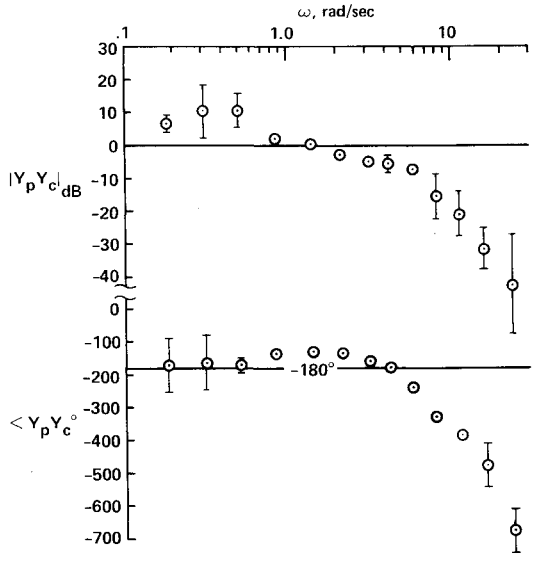

Fig. 7 Human-operator controlled-element transfer function for a single subject. Average of four runs. $Y_c = K/s^2$, delay = 0.0238 s.

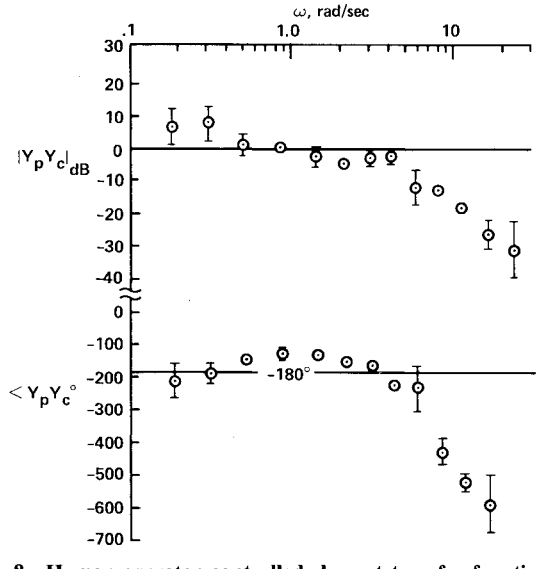

Fig. 8 Human-operator controlled-element transfer function for a single subject. Average of four runs. $Y_c = K/s^2$, delay = 0.357 s.

changes in relative remnant with delay do not appear to be significant. The remnant data does reflect the well-known decease in pilot linearity and stationarity when tracking controlled elements on the order of two or greater (e.g., K/s^2). The most noticeable effect of time delays across all of the controlled elements is the reduction in crossover frequency with increasing delay and the appearance of operator lead generation not attributable to the requirement of maintaining K/s-like pilot-vehicle characteristics in the frequency range around crossover. The crossover frequency regression is evident in Fig. 9, while the lead generation is implied in the slopes of the amplitude ratio curves of Figs. 3-8. There, broad frequency ranges appear with slopes less than the −20 dB/dec associated with K/s characteristics. These characteristics have been the cornerstone of all manual control theory and form the basis of the well-known "crossover" model of the human pilot.[8]

This deviation from the classical theory is particularly evident in Figs. 10 and 11, which illustrate experimentally derived Y_pY_c transfer functions for the $Y_c = K/s$ case with time delays of 0.0238 and 0.357 s, respectively. Note that in going from Fig. 10 to Fig. 11, the order of the internal model of the controlled-element dynamics in the structural-model fit changed from $k = 1$ to 2. This change was necessary to obtain an adequate fit to the experimental pilot-vehicle transfer function that showed an obvious first-order lead occurring below 1.0 rad/s in the case with the larger time delay. In terms of the internal model this change was somewhat surprising, since near the crossover frequency of 0.5 rad/s the phase-lag contribution of the 0.356 s time delay is only about 10 deg. In terms of the structural model then, the K/s controlled element with a 0.357 s time delay was compensated much like a K/s^2 controlled element! This analytical interpretation of pilot equalization was corroborated by an observation that the author made while the subjects tracked the K/s dynamics with the large time delay. Namely, the subjects exhibited the pulsive, "bang-bang" type of control activity long associated with controlled-element dynamics of second order.[11]

The lead generation evident in Fig. 11 also has a potentially deleterious effect on tracking performance. As Fig. 11 indicates, the amplitude ratio of the open-loop transfer function Y_pY_c becomes relatively flat over a broad frequency range. This means that a small increase in the pilot's gain can cause the crossover frequency to increase dramatically, with a concomitant decrease in phase margin. This point will be brought up again in what follows.

In terms of aircraft handling qualities, the dominant effect of the crossover frequency regression shown in Figs. 4, 6, 8, and 11 is in the degradation of closed-loop pilot-vehicle

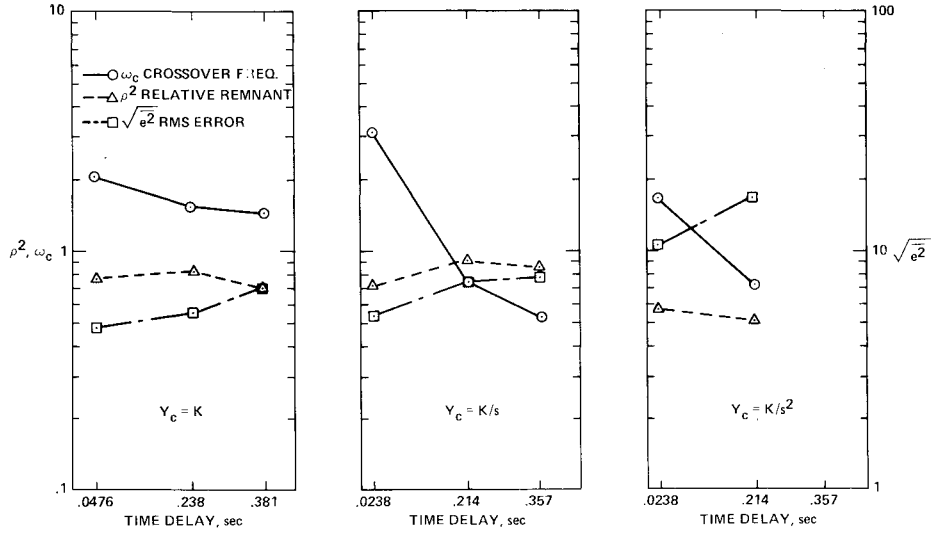

Fig. 9 Crossover frequency, relative remnant, and rms error scores for a single subject. Average of four runs.

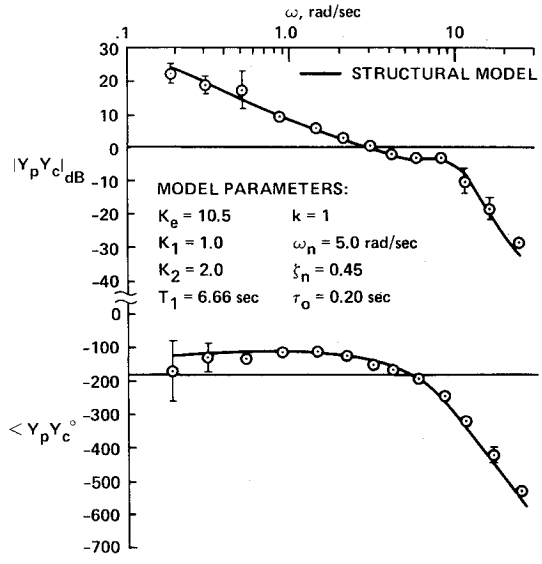

Fig. 10 Comparison of experimental and model transfer functions for a single subject. Experimental data from Fig. 5. $Y_c = K/s$, delay = 0.0238 s.

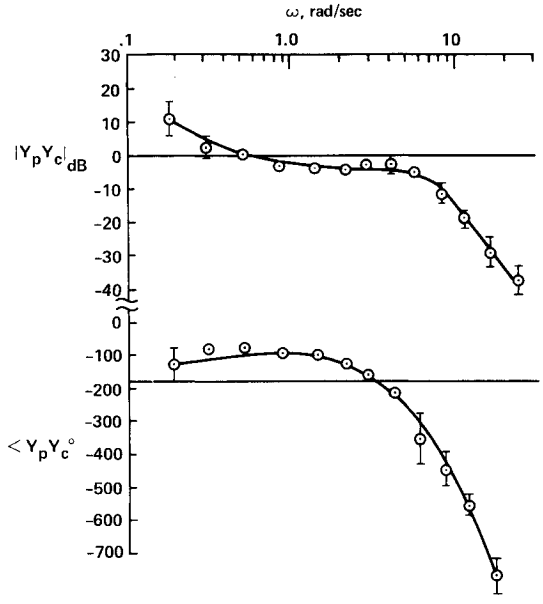

Fig. 11 Comparison of experimental and model transfer functions for a single subject. Experimental data from Fig. 6. $Y_c = K/s$, delay = 0.357 s.

response to abrupt, transient inputs. As an analytical means of demonstrating this, the closed-loop pilot-vehicle response (m/c in Fig. 1a) to a ramp input $[c(t) = t]$ was calculated using the measured pilot-vehicle transfer function Y_pY_c of Figs. 8 and 9 as

$$m(t) = \mathcal{L}^{-1}\left[\frac{1}{s^2}\frac{Y_pY_c(s)}{1+Y_pY_c(s)}\right] \tag{4}$$

This is not to imply that continuous, stochastic tracking models of the human pilot can be applied entirely to tracking deterministic inputs. Rather, when such inputs are embedded in random functions, as would be the case in aircraft piloting, the continuous models can provide useful information regarding pilot-vehicle response in the first few seconds after the input is initiated.

Figure 12 shows the ramp responses of Eq. (4). Note the significant performance differences. The sluggish response of

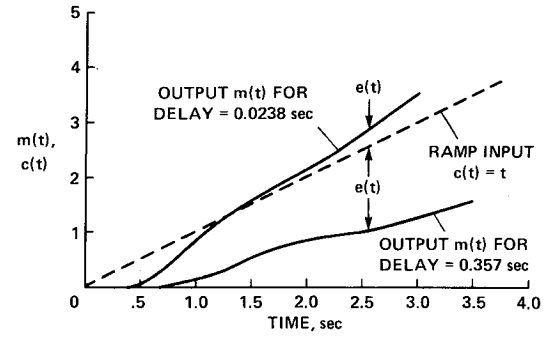

Fig. 12 Analytically derived ramp input responses for the system of Fig. 1a using Y_pY_c transfer functions of Figs. 5 and 6. $Y_c(s) = K/s$.

the system with large delay could catalyze a PIO in an aircraft since the pilot is very likely to increase his static gain and inadvertently drive the system phase margin to near zero[5] in an effort to improve the transient performance.

In terms of pilot equalization, lead generation has always been associated with increased levels of pilot workload.[13] Thus, aircraft control systems are, or at least should be, designed to obviate the necessity of lead generation on the part of the pilot. Traditionally, this has meant keeping the order of the vehicle dynamics less than two in the frequency range of crossover. The presence of significant time delays alters this situation, however. Comparing Figs. 10 and 11, one sees definite evidence of lead generation with the large delay even though the order of the system dynamics is unity. Indeed, the structural model fit indicates a lead time constant of 2.5 s! Similar results are obtained with the pure gain and second-order controlled elements. In the latter case, second-order lead generation on the part of the operator is apparent from the data.

Conclusions

The major conclusions to be drawn from this study are as follows.

1) Time delays can cause significant regression in pilot-vehicle crossover frequencies for a variety of controlled elements. This regression, which was analytically predicted in Ref. 5, has now been verified experimentally and has been hypothesized to be a major factor in the initiation of pilot-induced oscillations.

2) Time delays can result in significant pilot lead generation for a variety of controlled elements. Since pilot lead generation has been shown to contribute to pilot workload directly, a definite link between system time delays and pilot workload has been established.

References

[1] Stengel, R.F. and Miller, G.E., "Flight Tests of a Microprocessor Control System," *Journal of Guidance and Control*, Vol. 3, Nov.-Dec. 1980, pp. 494-500.

[2] Smith, R.E., Monagan, S.J., and Bailey, R.E., "An In-Flight Investigation of Higher Order Control Systems Effects in the Lateral-Directional Flying Qualities of Fighter Airplanes," AIAA Paper 81-1891, Aug. 1981.

[3] Berry, D.T., Powers, B.G., Szalai, K.J., and Wilson, R.J., "A Summary of an In-Flight Evaluation of Control System Pure Time Delays During Landing Using the F-8 DFBW Airplane," AIAA Paper 80-1626, Aug. 1980.

[4] Hodgkinson J. and Johnston, K.A., "Initial Results of an In-Flight Simulation of Augmented Dynamics in Fighter Approach and Landing," AIAA Paper 79-1783, Aug. 1979.

[5] Hess, R.A., "Analysis of Aircraft Attitude Control Systems Prone to Pilot-Induced Oscillations," *Journal of Guidance, Control, and Dynamics*, Vol. 7, Jan.-Feb. 1984, pp. 106-112.

[6]Hess, R.A., "A Structural Model of the Adaptive Human Pilot," *Journal of Guidance and Control,* Vol. 3, Sept.-Oct. 1980, pp. 416-423.

[7]Kleinman, D.L., Baron, S., and Levinson, W.H., "An Optimal Control Model of Human Response, Part I," *Automatica,* Vol. 6, 1970, pp. 357-369.

[8]McRuer, D.T., Graham, D. Krendel, E., and Reisener, W., Jr., "Human Pilot Dynamics in Compensatory Systems," AFFDL-TR-65-15, 1965.

[9]Richards, D. and Pilcher, C.D., "F/A-18A Initial Sea Trials," *The Society of Experimental Test Pilots Technical Review,* Vol. 16, No. 1, 1981, pp. 10-22.

[10]Franklin, G.F. and Powell, J.D., *Digital Control of Dynamic Systems,* Addison-Wesley, Reading, Mass., 1980.

[11]Hess, R.A., "A Rationale for Human Operator Pulsive Control Behavior," *Journal of Guidance and Control,* Vol. 2, May-June 1979, pp. 221-227.

[12]Hess, R.A., "Pursuit Tracking and Higher Levels of Skill Development," *IEEE Transactions on Systems, Man and Cybernetics,* Vol. SMC-11, April 1981, pp. 262-273.

[13]Hess, R.A., "A Model-Based Investigation of Manipulator Characteristics and Pilot/Vehicle Performance," *Journal of Guidance, Control, and Dynamics,* Vol. 6, Sept.-Oct. 1983, pp. 348-354.

[14]McDonnell, J.D., "Pilot Rating Techniques for the Estimation and Evaluation of Handling Qualities," AFFDL-TR-68-76, 1968.